Universidade Estadual de Campinas

Instituto de Física Gleb Wataghin

Yago Barbosa de Godoy

Efeitos de desordem em modelos tipo Kitaev

Disorder effects on Kitaev models

Campinas
2020

YAGO BARBOSA DE GODOY

Disorder effects on Kitaev models

Efeitos de desordem em modelos tipo Kitaev

Dissertação apresentada ao Instituto de Física Gleb Wataghin da Universidade Estadual de Campinas como parte dos requisitos exigidos para a obtenção do título de Mestre em Física, na área de Física.

Dissertation presented to the Instituto de Física Gleb Wataghin of the University of Campinas in partial fulfillment of the requirements for the degree of Master, in the area of physics.

Supervisor/Orientador: EDUARDO MIRANDA

ESTE EXEMPLAR CORRESPONDE À VERSÃO
FINAL DA DISSERTAÇÃO DEFENDIDA PELO ALUNO
YAGO BARBOSA DE GODOY, E ORIENTADA PELO
PROF. DR. EDUARDO MIRANDA.

CAMPINAS
2020

Ficha catalográfica
Universidade Estadual de Campinas
Biblioteca do Instituto de Física Gleb Wataghin
Lucimeire de Oliveira Silva da Rocha - CRB 8/9174

G548d

Godoy, Yago Barbosa de, 1994-
Disorder effects on Kitaev models / Yago Barbosa de Godoy. – Campinas, SP : [s.n.], 2020.

Orientador: Eduardo Miranda.
Dissertação (mestrado) – Universidade Estadual de Campinas, Instituto de Física Gleb Wataghin.

1. Kitaev, Modelo de. 2. Férmions. 3. Quase-partículas (Física). 4. Grupo de renormalização. 5. Líquidos quânticos. I. Miranda, Eduardo, 1963-. II. Universidade Estadual de Campinas. Instituto de Física Gleb Wataghin. III. Título.

Informações para Biblioteca Digital

Título em outro idioma: Efeitos de desordem em modelos tipo Kitaev
Palavras-chave em inglês:
Kitaev model
Fermions
Quasiparticles (Physics)
Renormalization group
Quantum liquids
Área de concentração: Física
Titulação: Mestre em Física
Banca examinadora:
Eduardo Miranda [Orientador]
Ricardo Luís Doretto
André de Pinho Vieira
Data de defesa: 08-06-2020
Programa de Pós-Graduação: Física

Identificação e informações acadêmicas do(a) aluno(a)
- ORCID do autor: https://orcid.org/0000-0002-3105-9078
- Currículo Lattes do autor: http://lattes.cnpq.br/5727030927823104

MEMBROS DA COMISSÃO JULGADORA DA DISSERTAÇÃO DE MESTRADO DE **YAGO BARBOSA DE GODOY – RA 148247** APRESENTADA E APROVADA AO INSTITUTO DE FÍSICA "GLEB WATAGHIN", DA UNIVERSIDADE ESTADUAL DE CAMPINAS, EM 08 / 06 / 2020.

-COMISSÃO JULGADORA:

- Prof. Dr. Eduardo Miranda – Orientador – DFMC/IFGW/UNICAMP

- Prof. Dr. Ricardo Luís Doretto - DFMC/IFGW/UNICAMP

- Prof. Dr. André de Pinho Vieira - IF/USP

OBS.: Ata da defesa com as respectivas assinaturas dos membros encontra-se no SIGA/Sistema de Fluxo de Dissertação/Tese e na Secretaria do Programa da Unidade.

CAMPINAS

2020

AGRADECIMENTOS

Aos meus pais que, mesmo não entendendo o porquê de seguir na física, sempre me apoiaram incondicionalmente por todos esses anos e me incentivaram a dar o melhor de mim.
Ao professor Eduardo Miranda pela oportunidade e por ter feito muito mais do que o papel de um orientador. Muito obrigado pelas discussões e ensinamentos, que me ajudaram a crescer tanto quanto pesquisador, quanto pessoa. Obrigado pela amizade ao longo desses anos.
Ao professor Ricardo Doretto pela amizade, pela didática ímpar e por ser sempre tão receptivo e disposto nas inúmeras vezes que bati à sua porta no DFMC.
Aos professores Marcus Bonança e Mário Tamashiro pelas discussões estimulantes e por se mostrarem tão prestativos.
Aos meus grandes amigos Carlos, Gabriel e Pedro que me acompanham desde antes mesmo da graduação, e mesmo sem entender absolutamente nada do que eu faço estão sempre torcendo por mim, às vezes, literalmente, aos gritos. Obrigado pelo apoio incondicional.
Ao Alexssandre, o qual tive a felicidade de conhecer durante o mestrado. Obrigado pela amizade, companheirismo, e pelas madrugadas acordados resolvendo as listas de mecânica quântica.
Ao Murilo pela amizade e pela incrível tranquilidade contagiante.
Ao Mário pelas diversas vezes nas quais o busquei com alguma dúvida burocrática e ele tão prontamente respondeu.
Aos meus irmãos, que me aguentaram por todos esses anos e mesmo sem perceberem, fizeram de mim uma pessoa melhor.
À toda minha família e todos meus amigos ao longo desses anos, meu sincero obrigado.
À Mariana que esteve ao meu lado ao longo de todo esse trajeto de mestrado, me apoiando mesmo nos momentos mais difíceis e sempre me empurrando para frente.
Ao meu grande amigo Rodrigo, "Harry", sempre disponível e com um sorriso no rosto, nos momentos fáceis e nos momentos difíceis. Te conhecer me fez uma pessoa melhor.
O presente trabalho foi realizado com apoio da Coordenação de Aperfeiçoamento de Pessoal de Nível Superior - Brasil (CAPES) - Código de Financiamento 001.

ABSTRACT

The purpose of this work is to study the effects of disorder on the Majorana honeycomb model. We did so for two different initial flux configurations, one which corresponds to the sector containing the ground state, i.e., the zero flux sector, and a configuration which corresponds to highly excited states, namely the random flux configuration. The method chosen for the study of these systems was the Strong Disorder Renormalization Group (SDRG). Our findings suggest that for the initial configuration corresponding to the zero flux sector, the Majorana honeycomb model is shielded against weak disorder, whereas the system always flows to infinite disorder given that the initial disorder is strong enough. As for the random flux initial configuration, we believe that the system always flows to infinite disorder, with a tunnelling exponent $\psi = \frac{1}{2}$.

RESUMO

O objetivo deste trabalho é estudar os efeitos de desordem no modelo hexagonal de férmions de Majorana. Isso foi feito para duas configurações iniciais de fluxo distintas: uma correspondente ao setor que contém o estado fundamental, chamado de setor de fluxo zero; e outra que contém estados altamente excitados, chamada de configuração de fluxo aleatório. O método utilizado para o estudo desses sistemas foi o Grupo de Renormalização de Desordem Forte (GRDF). Nossos dados sugerem que a rede hexagonal de Majoranas na configuração inicial de fluxo zero é blindada contra desordem fraca, enquanto o sistema sempre flui para desordem infinita uma vez que a desordem inicial é forte o suficiente. Já para a configuração inicial de fluxo aleatório, acreditamos que o sistema sempre flui para a desordem infinita, com um expoente de tunelamento $\psi = \frac{1}{2}$.

TABLE OF CONTENTS

Agradecimentos 5
Abstract 6
Resumo 7
Table of Contents 8
Chapter I: Introduction 9
Chapter II: The Kitaev Model 14
2.1 Majorana operators 16
2.2 Application to the model 17
2.3 The energy ground state 20
2.4 The Majorana Honeycomb model and the implementation of disorder 21
Chapter III: Strong Disorder Renormalization Group 23
3.1 The SDRG and the 1/2-spin Heisenberg chain 23
3.2 The Majorana Honeycomb SDRG 28
Chapter IV: Algorithm and results 34
4.1 The zero flux sector 34
4.2 The random flux regime 41
4.3 The square lattice 45
Chapter V: Conclusions 47
Appendix A: How α relates to disorder 48
Bibliography 49

Chapter 1

INTRODUCTION

Magnetic systems have been known for many centuries. However, our comprehension about them has increased significantly with the advent of quantum mechanics. This is due to the fact that the primary origin of magnetism lies in the intrinsic angular momentum carried by particles, which came to be known as spin. We know today that most magnetic materials present some kind of spin ordering, which in turn dictates the physical properties of the material. Therefore, the interaction between spins is a central theme in the study of magnetic systems, for it is the primary source of magnetic ordering.

Many models have thus been proposed to describe these interactions. Two very famous and widely used ones are the Heisenberg Model and the Ising Model. Both can be described by an exchange interaction, a phenomenon arising between identical particles, which is a consequence of the Coulomb interaction between electrons and the exchange symmetry present in the wave function that describes them. The Ising model is the simpler one, for it considers all spins in the system to be in either one of two states, +1 or −1, corresponding to the two values of a spin component, say, S_z. In the absence of an external magnetic field, the Hamiltonian of the model is

$$H = -\sum_{\langle ij \rangle} J\sigma_i\sigma_j,$$

where J is the coupling constant, the sum $\langle ij \rangle$ is over all nearest neighbours, and $\sigma_i = \pm 1$. As for the Heisenberg model, the Hamiltonian in the absence of an external field is

$$H = -\sum_{\langle ij \rangle} J\overrightarrow{S_i}\cdot\overrightarrow{S_j},$$

where now $\overrightarrow{S_i}$ is the spin operator associated with site i. For a spin-$\frac{1}{2}$ system, $\overrightarrow{S_i}$ would simply be the Pauli spin-$\frac{1}{2}$ matrices times $\frac{\hbar}{2}$. The spin configuration which minimizes each interaction for both models is the one where neighbouring spins are either parallel when $J > 0$, or antiparallel when $J < 0$. This explains the behaviour

some materials show, in which spins have a tendency of aligning as temperature is lowered and the system's energy is decreased. These materials are said to exhibit ferromagnetic behaviour if spins tend to align in a parallel manner, whereas they are said to exhibit antiferromagnetic behaviour if spins tend to be antiparallel.

However, a magnetic system may not always be able to minimize all exchange interactions simultaneously in its ground state, as is the case of the spin-$\frac{1}{2}$ antiferromagnetic Ising model on the triangular lattice. If one sets two spins on the corners of a triangle in an antiparallel manner so as to minimize their exchange interaction, there is no possible orientation for the third one which minimizes its interactions with the other two (figure 1.1). The system is then said to be geometrically frustrated, for this phenomenon is inextricably linked to lattice geometry.

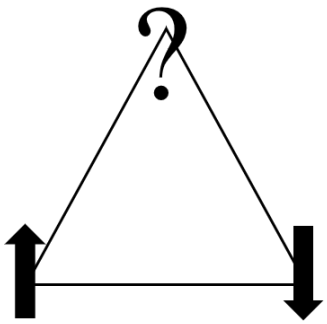

Figure 1.1: Depiction of interacting spins in a triangular arrangement. There is no possible configuration for which all three interactions are minimized.

Given that the exchange interactions can no longer be simultaneously satisfied, frustration in a system acts as to destroy magnetic ordering. This led Anderson, when studying the spin-$\frac{1}{2}$ antiferromagnetic Heisenberg model on the triangular lattice in 1973, to propose the existence of systems completely devoid of magnetic ordering even in their ground state, due to geometrical frustration along with quantum fluctuations, which also act as to destroy order. He suggested that the ground state would instead be composed of a quantum superposition of different pairings of spins into singlets, which he called a Resonating Valence Bond (RVB) state (figure 1.2) (Anderson, 1973).

Since, by definition, there would be quantum mechanical fluctuations of the valence bonds, the term Quantum Spin Liquid (QSL) was coined, as opposed to

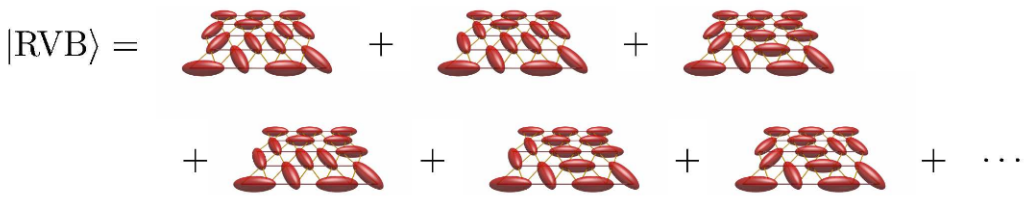

Figure 1.2: The RVB state as proposed by Anderson. It is defined as a superposition of different pairings of spins into singlets. Illustration as seen in (Savary and Balents, 2016).

solids with localized static bonds (Balents, 2010). It was not until 1987 that the QSL theory became the subject of intense physical interest, when Anderson argued that the QSL theory could underlie the physics of the then recently discovered high-temperature superconductors (Anderson, 1987), (Bednorz and Müller, 1986). Yet, due to the difficulty in proving whether a state truly possessed some kind of magnetic ordering in the low energy limit, the QSL theory did not show important theoretical improvements.

However, in 2006, Kitaev proposed the first model in which the ground state is exactly solvable and predicts both gapless and gapped QSL phases depending on the exchange coupling constants (Kitaev, 2006). Moreover, the model predicts the fractionalization of spins into emergent quasiparticles, the Majorana fermions. These particles date back to 1937, when Ettore Majorana showed that the Dirac equation accepts a class of solutions that describes particles that are identical to their antiparticles (Majorana, 1937). Although this may seem highly theoretic, materials which present QSL states have been widely searched for, and some probable candidates have been found, as is the case for $\alpha - RuCl_3$ (Banerjee et al., 2016). A list of probable candidates has also been presented by Balents (Balents, 2010) and more recently by Savary (Savary and Balents, 2016). Experimental evidence for the Majorana fermion has also been presented (He et al., 2017).

Now, in the context of magnetic ordering, it is important to understand the effects of disorder in a system, for it can play a dominant role over quantum and thermal fluctuations, and thus give rise to completely new phenomena, such as the Anderson localization (Anderson, 1958).

A very powerful method often used to study the critical behaviour of many-body systems near a phase transition is the Renormalization Group (RG). The basic idea

behind the RG is to reduce the complexity of a many-body system by gradually integrating out large energy (short wave length) degrees of freedom and analysing how the left-over degrees of freedom are effectively described. When the coefficients of the interaction terms describing the low-energy (long wave length) sector start to converge as the energy scale is lowered, we say we have found a fixed point. From the properties of the fixed point and its vicinity, we can extract physical properties of the system (M. E. Fisher, 1974). Moreover, the dependence of these coefficients on the lowering energy scale are usually described by differential equations called the RG flow equations.

However, the difficulty in formulating a renormalization group theory which in turn quantifies the physical properties of a disordered system lies in the fact that renormalizations in disordered systems involve probability distributions, whereas in pure systems they usually involve a finite number of coupling constants. This complicates the analysis of the RG flow and the determination of the fixed points. It is in this context that the Strong Disorder Renormalization Group (SDRG), introduced by Ma, Dasgupta and Hu, was proven to be so valuable. The method was first proposed in order to study the low energy physics of a spin-$\frac{1}{2}$ antiferromagnetic Heisenberg chain in the presence of disorder (Ma, Dasgupta, and Hu, 1979). Whereas the method was first considered to be an approximate procedure, Fisher showed analytically that the renormalization flow converges towards an infinite disorder fixed point, meaning the method is asymptotically exact (D. S. Fisher, 1994). The method has since then been applied with great success to a variety of different disordered systems (Iglói and Monthus, 2005), (Kovács and Iglói, 2011), (Quito, Hoyos, and Miranda, 2016).

In this context, it would be very interesting to study the effects of disorder on the Kitaev model. The implementation of the SDRG for this model is, however, extremely complicated, one of the reasons being that the renormalization procedure may end up changing the initial flux configuration, which in turn defines the accessible energy states. Given the complications, we set ourselves to study the effects of disorder on a Majorana honeycomb model, a "toy model" inspired by the Kitaev one. This particular model raises the question of Anderson localization in a Majorana fermion system, which has not been studied yet. We take a step in that direction.

I start this thesis by introducing the Kitaev model and presenting the ground state solution. Then we introduce the SDRG method, which was the method of choice to study the desired systems. More specifically, for pedagogic reasons, I shall present the SDRG when applied to the spin-$\frac{1}{2}$ antiferromagnetic Heisenberg chain in the presence of disorder. Afterwards, we discuss the SDRG method when applied to the Majorana honeycomb model, and lastly, I present the computational method and the obtained results. We then end this dissertation with some conclusions and future prospects.

Chapter 2

THE KITAEV MODEL

Kiatev's model is defined on a hexagonal lattice with a spin-$\frac{1}{2}$ located at each of the vertices. The hexagonal lattice can in turn be seen as two triangular Bravais lattices, referred to as "even" and "odd" (the empty and full circles in figure 2.1), thus one unit cell of the lattice contains one vertex of each kind.

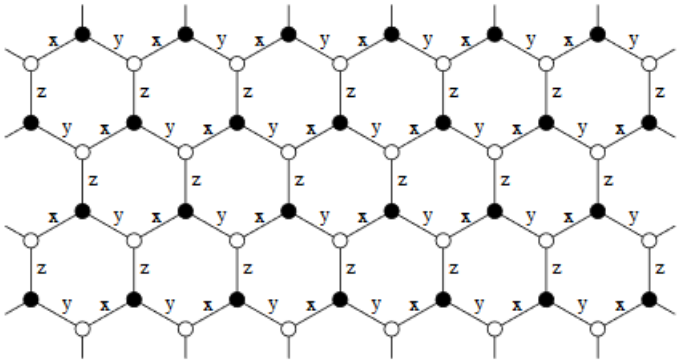

Figure 2.1: The hexagonal lattice. Each site is connected to its three first neighbours. The links are divided in three types, depending on their direction, "x-links", "y-links", and "z-links".

The idea is to construct such a Hamiltonian that the interactions along nearest neighbouring bonds cannot be satisfied simultaneously, giving rise to frustration, which could drive the system into a quantum spin liquid (QSL), while having it be exactly solvable for the ground state. The Hamiltonian is as follows:

$$H = -J_x \sum_{x-links} \sigma_j^x \sigma_k^x - J_y \sum_{y-links} \sigma_j^y \sigma_k^y - J_z \sum_{z-links} \sigma_j^z \sigma_k^z, \tag{2.1}$$

where σ_j^a is a Pauli's matrix in the a direction on site j and J_a are model parameters.

What we wish to do now is to find constants of motion in which subspaces' the Hamiltonian can be diagonalized. Kitaev starts by defining the following plaquette operators:

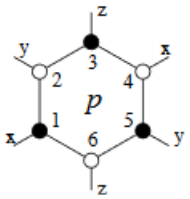

$$W_p = \sigma_1^x \sigma_2^y \sigma_3^z \sigma_4^x \sigma_5^y \sigma_6^z, \tag{2.2}$$

where p labels the plaquette. From the Pauli matrices definition, it follows that

$$[\sigma_j^a, \sigma_k^b] = 2i\epsilon_{abc}\sigma_k^c \delta_{j,k}, \tag{2.3}$$

which in turn implies that

$$[W_p, W_p'] = 0, \quad [H, W_p] = 0. \tag{2.4}$$

Therefore, the W_p form a set of constants of motion which commute between themselves.

It also follows from the Pauli matrices definition that

$$\sigma_x^2 = \sigma_y^2 = \sigma_z^2 = 1, \tag{2.5}$$

and hence $W_p^2 = 1$. Thus,

$$W_p = \pm 1 \tag{2.6}$$

are the eigenvalues of W_p; hence the Hilbert space can be decomposed in well defined subspaces of W_p.

Our goal is then to rewrite Hamiltonian (2.1) in terms of the W_p operators, so that the Hamiltonian can be promptly diagonalized. Notice however, that an interaction along a specific direction i, $i = x, y, z$, depends only of σ^i, whereas $W_p = \sigma_1^x \sigma_2^y \sigma_3^z \sigma_4^x \sigma_5^y \sigma_6^z$. What follows next is a convenient, particular representation of the spin operators in terms of Majorana operators. This results in a Hamiltonian which is quadratic in form and thus makes an exact solution possible.

2.1 Majorana operators

In 1937, Ettore Majorana showed that the Dirac equation accepts a class of solutions that describes particles that are identical to their antiparticles. These particles are called Majorana fermions, meaning they are spin-$\frac{1}{2}$ particles whose creation and annihilation operators are precisely the same. We can construct a particular representation in terms of the usual fermionic operators in the following manner:

$$f_j = a_j + a_j^\dagger, \qquad g_j = \frac{a_j - a_j^\dagger}{i}, \tag{2.7}$$

where a and $a^\dagger$ are the usual spin-$\frac{1}{2}$ creation and annihilation operators. Note that any fermion can be written as a combination of two Majorana fermions, which is analogous to splitting the fermion into a real and an imaginary part, each of which is a distinct Majorana fermion (Wilczek, 2009).

Thus, instead of the usual description of a system with n fermionic modes that is done by n creation and annihilation operators $a_k^\dagger, a_k$, $(k = 1, ..., n)$, one can instead opt to use $2n$ Majorana operators.

By definition we see that:

$$f_j = f_j^\dagger, \quad g_j = g_j^\dagger, \tag{2.8}$$

$$f_j^2 = g_j^2 = 1, \tag{2.9}$$

$$\{f_j, f_j\} = \{g_j, g_j\} = 2, \tag{2.10}$$

$$\{f_j, g_j\} = 0. \tag{2.11}$$

It also follows immediately from the definition (2.7) how the Majorana operators act on the Hilbert space:

$$f|0\rangle = (a + a^\dagger)|0\rangle = |1\rangle, \tag{2.12}$$

$$g|0\rangle = \frac{a - a^\dagger}{i}|0\rangle = i|1\rangle, \tag{2.13}$$

$$f|1\rangle = |0\rangle, \tag{2.14}$$

$$g|1\rangle = -i|0\rangle. \tag{2.15}$$

Here, $|0\rangle$ represents the usual spin-$\frac{1}{2}$ vacuum and $|1\rangle = a^\dagger|0\rangle$.

2.2 Application to the model

We wish to rewrite Hamiltonian (2.1) in such a way that it can be readily diagonalized. To do that, we start by representing the spin operators σ^x, σ^y, and σ^z in terms of Majorana operators: $\sigma^x \to \tilde{\sigma}^x$, $\sigma^y \to \tilde{\sigma}^y$, and $\sigma^z \to \tilde{\sigma}^z$. The following particular representation for a spin is chosen:

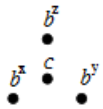

$$\tilde{\sigma}^x = ib^x c, \;\; \tilde{\sigma}^y = ib^y c, \;\; \tilde{\sigma}^z = ib^z c, \tag{2.16}$$

where b^x, b^y, b^z, c are four Majorana operators. Also, each spin is depicted by 4 Majorana fermions, as is shown in figure (2.2).

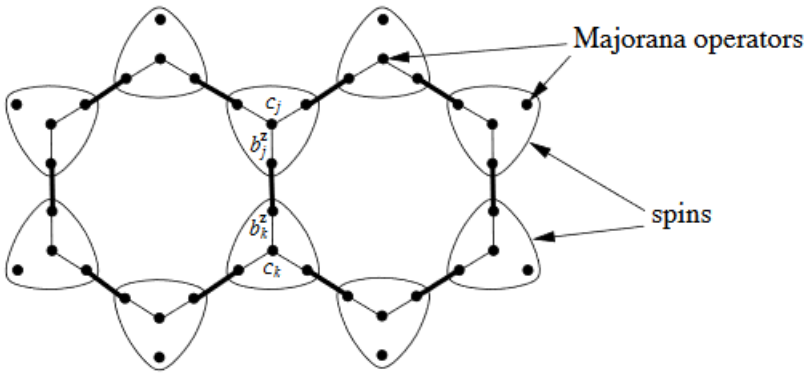

Figure 2.2: Graphic depiction of the Majorana operators representing a spin.

This new representation is not arbitrary, however. It is necessary that all algebraic properties of the Pauli matrices are maintained. Nonetheless, there is yet another complication. The spin-$\frac{1}{2}$ is defined in a 2-dimensional Hilbert space, whereas the four Majorana operators described in (2.16) act on the 4-dimensional Hilbert space, hence by changing the representation we are introducing new states to the system which do not correspond to physical states. Therefore, we define the constraint

$$D = b^x b^y b^z c, \tag{2.17}$$

such that

$$\left(\frac{1+D}{2}\right)|\psi\rangle = |\psi\rangle \tag{2.18}$$

acts as a projector into the physical subspace, if and only if $D = 1$. Indeed, following equations (2.9) and (2.11) we see that $D^2 = 1$, thus

$$D = \pm 1. \tag{2.19}$$

Now, by setting $D = 1$ and returning to Eq. (2.16), one can see that

$$[\tilde{\sigma}_j^a, \tilde{\sigma}_k^b] = 2i\epsilon_{abc}\tilde{\sigma}_k^c \delta_{j,k}, \tag{2.20}$$

$$(\tilde{\sigma}_j^a)^\dagger = \tilde{\sigma}_j^a, \tag{2.21}$$

$$(\tilde{\sigma}_j^a)^2 = 1. \tag{2.22}$$

$$\tilde{\sigma}^x\tilde{\sigma}^y\tilde{\sigma}^z = ib^x b^y b^z c = iD = i. \tag{2.23}$$

Hence, **only** in the subspace defined by $D = 1$, all original algebraic properties of the Pauli matrices are satisfied. Such a result implies that we can work in the extended space for practical reasons and use our constraint $D = 1$ to obtain only physical states.

Finally, we make the substitution $\sigma_j^a \rightarrow \tilde{\sigma}_j^a$ and rewrite Hamiltonian (2.1) in terms of the Majoranas:

$$\tilde{H} = \frac{i}{2}\sum_{j,k} J_{\alpha_{jk}} \hat{u}_{jk} c_j c_k, \tag{2.24}$$

where

$$\hat{u}_{jk} = ib_j^{\alpha_{jk}} b_k^{\alpha_{jk}}, \tag{2.25}$$

$$\alpha_{jk} = x, y, z \quad \text{depending on the direction of the link.} \tag{2.26}$$

The factor $\frac{1}{2}$ accounts for the fact that each pair of connected sites is counted twice.

It is interesting to write $\tilde{H}$ in terms of $\hat{u}_{jk}$ due to the fact that:

$$(\hat{u}_{jk})^2 = 1 \qquad \rightarrow \qquad u_{jk} = \pm 1, \tag{2.27}$$

$$[\tilde{H}, \hat{u}_{jk}] = 0, \tag{2.28}$$

hence we can diagonalize Hamiltonian (2.24) in well defined subspaces of $u_{jk} = \pm 1$.

There is still however a complication. For our solutions to correspond to physical states, we need to impose the constraint $D = 1$. Yet,

$$[\hat{u}_{jk}, D_j] \neq 0, \tag{2.29}$$

thus it is of no use to indeed diagonalize $\tilde{H}$ in subspaces of $\hat{u}_{jk}$. Let us instead define the following operator:

$$\tilde{W}_p = \prod_{plaquette} \hat{u}_{jk} \qquad (j \in \text{even sublattice}, k \in \text{odd sublattice}). \tag{2.30}$$

For this operator, on the other hand, we see that

$$[\tilde{W}_p, \tilde{H}] = 0, \tag{2.31}$$

$$[\tilde{W}_p, D_j] = 0. \tag{2.32}$$

This means that the invariant physical states of the problem can be described in terms of the variables $\tilde{W}_p$, which we will have a better understanding of next.

I shall be a little more mathematically thorough in what comes next due to the fact that I couldn't quite understand why $\tilde{W}_p$ was defined in this manner the first time I read Kitaev's paper. For simplicity reasons, from hereafter the hats will be omitted, i.e. $\hat{u} = u$. For an arbitrary plaquette,

$$\tilde{W}_p = u_{21}\, u_{23}\, u_{43}\, u_{45}\, u_{65}\, u_{61}.$$

Following equation (2.25) and the schematics from (2.2), we have that

$$\tilde{W}_p = i b_2^z b_1^z\, i b_2^x b_3^x\, i b_4^y b_3^y\, i b_4^z b_5^z\, i b_6^x b_5^x\, i b_6^y b_1^y.$$

Rearranging the terms in accordance with eq. (2.11)

$$\tilde{W}_p = b_1^y\, b_2^z\, b_3^x\, b_4^y\, b_5^z\, b_6^x\, b_1^z\, b_2^x\, b_3^y\, b_4^z\, b_5^x\, b_6^y.$$

Using Eq. (2.9) and rearranging the terms so that same site operators are next to each other

$$\tilde{W}_p = -\,\tilde{\sigma}_1^y\,\tilde{\sigma}_1^z\,\tilde{\sigma}_2^z\,\tilde{\sigma}_2^x\,\tilde{\sigma}_3^x\,\tilde{\sigma}_3^y\,\tilde{\sigma}_4^y\,\tilde{\sigma}_4^z\,\tilde{\sigma}_5^z\,\tilde{\sigma}_5^x\,\tilde{\sigma}_6^x\,\tilde{\sigma}_6^y. \tag{2.33}$$

Here is when it all comes together. We know from Eqs. (2.20) - (2.23) that in the subspace defined by $D = 1$, the Majorana spin representation obey all the properties shared by the Pauli matrices, and therefore this subspace corresponds to the physical subspace. But how does this condition affect equation (2.33)? Let us look at Eq. (2.23):

$$\tilde{\sigma}_j^x\tilde{\sigma}_j^y\tilde{\sigma}_j^z = i.$$

From Eq. (2.22) we know that $(\tilde{\sigma}_j^a)^2 = 1$. Therefore

$$\tilde{\sigma}_j^x\tilde{\sigma}_j^y = i\tilde{\sigma}_j^z. \tag{2.34}$$

Note that this is **only** true because we set $D = 1$. Substituting Eq. (2.34) on Eq. (2.33) we finally get:

$$\tilde{W}_p = \tilde{\sigma}_1^x\tilde{\sigma}_2^y\tilde{\sigma}_3^z\tilde{\sigma}_4^x\tilde{\sigma}_5^y\tilde{\sigma}_6^z, \tag{2.35}$$

which is precisely Eq. (2.2) when we make the substitution $\sigma_j^a \rightarrow \tilde{\sigma}_j^a$. In other words, when we set $D = 1$

$$\tilde{W}_p = W_p. \tag{2.36}$$

Thus, by making $\tilde{W}_p = W_p$ in each and every plaquette, we can work in the expanded space with $\tilde{W}_p$ while having an accurate representation of the physical state.

2.3 The energy ground state

We are interested in studying the low energy limit, so the ground state is particularly of interest. It follows from a theorem proved by Lieb, that the energy minimum is achieved when $W_p = 1$ for all p (Lieb, 1994). This configuration corresponds to a vortex-free field regime, and is thus called the zero flux configuration. Consequently, we may assume $u_{jk} = 1$ for all links, where j belongs to the even sublattice and k belongs to the odd sublattice. This field configuration is such that the system now presents a translational symmetry and therefore the fermionic spectrum can

be obtained analytically by the means of a Fourier transform applied to the now quadratic Hamiltonian

$$\tilde{H} = \frac{i}{2}\sum_{j,k} J_{\alpha_{jk}} c_j c_k, \tag{2.37}$$

where we set $u_{jk} = 1$ for all j, k. The obtained spectrum is

$$\epsilon(\mathbf{q}) = \pm|f(\mathbf{q})|, \tag{2.38}$$

where

$$f(\mathbf{q}) = 2(J_x e^{i(\mathbf{q},\mathbf{n_1})} + J_y e^{i(\mathbf{q},\mathbf{n_2})} + J_z), \tag{2.39}$$

and

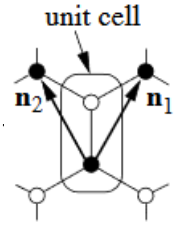

$$\mathbf{n_1} = (\frac{1}{2}, \frac{\sqrt{3}}{2}), \qquad \mathbf{n_2} = (-\frac{1}{2}, \frac{\sqrt{3}}{2}) \tag{2.40}$$

is the chosen basis of the translation group in the xy-coordinates.

From equation (2.38), an important property of the spectrum can be obtained. If $\epsilon(\mathbf{q}) = 0$ for some $\mathbf{q}$, the spectrum is found the be gapless. It follows from Eq. (2.39) that the spectrum is gapless if and only if $|J_x|$, $|J_y|$, $|J_x|$ satisfy the triangle inequalities:

$$|J_x| \leq |J_y| + |J_z|, \qquad |J_y| \leq |J_x| + |J_z|, \qquad |J_z| \leq |J_x| + |J_y|. \tag{2.41}$$

This is illustrated in figure (2.3).

2.4 The Majorana Honeycomb model and the implementation of disorder

It is known that the presence of disorder in a system can give rise to completely new phenomena, such as the Griffith's phase (Griffiths, 1969). With that in mind and inspired on the Kitaev model, we set ourselves to study the effects of disorder on a Majorana honeycomb model. Instead of a spin-$\frac{1}{2}$, each site of figure (2.1) is

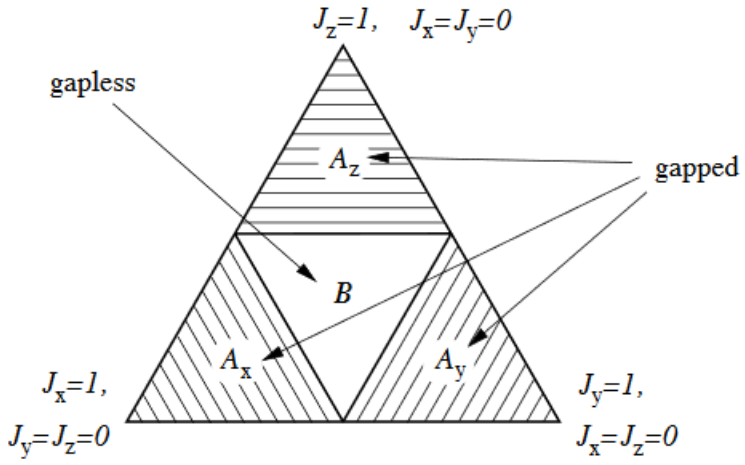

Figure 2.3: Phase diagram of the model (2.37). The region defined by inequalities (2.41) are marked by B.

now filled with a Majorana fermion and their interaction is analogous to that which was found for the Kitaev model in terms of the Majoranas:

$$\boxed{H = \sum_{n.n.} t_{j,k}\, u_{j,k}\, \eta_j\, \eta_k,} \tag{2.42}$$

where the sum is done over the nearest neighbours and here $u_{j,k}$ simply states the direction which the bond takes. The implementation of disorder was done by generating random values for the coupling constants $t_{j,k}$ according to some distribution $P(t)$, and the Majorana operators are now represented by η_i.

We started by fixing $W_p = 1$ for all p and thus studying such a system whose **initial configuration** is analogous to that of the Kitaev model in the zero flux sector. For this reason, we shall refer to it as the Majorana honeycomb model in the zero flux sector. We then proceeded to let $W_p = \pm 1$ be randomly and uniformly distributed. For this study, our method of choice was the Strong Disorder Renormalization Group (SDRG). Afterwards, we applied the same method to a Majorana square lattice for comparison. An isotropic distribution of $t_{j,k}$ was chosen in all cases.

Chapter 3

STRONG DISORDER RENORMALIZATION GROUP

We now present the Strong Disorder Renormalization Group (**SDRG**) theory, a method which was firstly introduced by Ma, Dasgupta and Hu in order to study a spin-$\frac{1}{2}$ antiferromagnetic Heisenberg chain in the presence of disorder. This method allows us to determine the physics of a many-body system at a specific energy scale. It was designed to facilitate the study of a system in the low energy limit and consists of decimations in real space of the highest value of a random variable. We shall start by illustrating the method when applied to the spin-$\frac{1}{2}$ Heisenberg chain for didactic reasons, and then apply it to the Majorana honeycomb model.

3.1 The SDRG and the 1/2-spin Heisenberg chain

The Heisenberg model for a spin-$\frac{1}{2}$ antiferromagnetic chain in the absence of an external field is described by the Hamiltonian

$$H = \sum_i J_i \boldsymbol{S}_i \cdot \boldsymbol{S}_{i+1}, \tag{3.1}$$

where S_i is the spin operator indexed to site i, and $J_i > 0$ is the coupling constant between spins S_i and S_{i+1}. The disorder is introduced by letting all J_i be independent random variables distributed according to some distribution $P(J)$, as is illustrated in figure (3.1).

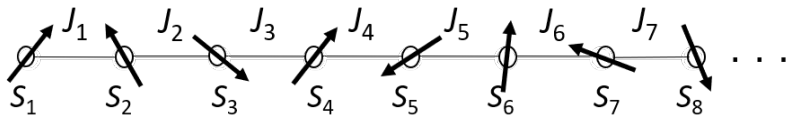

Figure 3.1: spin-$\frac{1}{2}$ antiferromagnetic chain.

The idea now is to reduce the degrees of freedom of a spin through the pairing with another spin in a singlet state. The procedure is as follows:
(i) We first find the highest energy coupling in the chain, $\Omega = \max\{J_i\}$, e.g. $\Omega = J_2$.
(ii) We now consider the interaction between $\boldsymbol{S}_2$ and $\boldsymbol{S}_3$ as much more significant than that of $\boldsymbol{S}_1$ with $\boldsymbol{S}_2$ and that of $\boldsymbol{S}_3$ with $\boldsymbol{S}_4$, which is justifiable on highly disordered systems. In other words, we take

$$H_1 = J_1 \boldsymbol{S}_1 \cdot \boldsymbol{S}_2 + J_3 \boldsymbol{S}_3 \cdot \boldsymbol{S}_4, \tag{3.2}$$

as a perturbation of

$$H_0 = J_2 \boldsymbol{S}_2 \cdot \boldsymbol{S}_3. \tag{3.3}$$

The ground state of H_0 is a singlet state, so let us suppose that the energy of the highest coupling in the system is much greater than the temperature T, temperature in which we wish to determine the thermodynamic properties of the system, i.e. $J_2 = \Omega \gg T$. This means that the triplet state of the Hamiltonian H_0 is very unlikely to be thermically accessed. This justifies our next step.
(iii) We remove S_2 and S_3 from the system and let S_1 and S_4 interact effectively in accordance with

$$H^{\text{eff}} = \tilde{J} \boldsymbol{S}_1 \cdot \boldsymbol{S}_4, \qquad \tilde{J} = \frac{J_1 J_2}{2\Omega}, \tag{3.4}$$

where $\tilde{J}$ is obtained after a second order correction to Hamiltonian (3.3). This means that the strongly correlated singlet pair, spins 2 and 3, have been frozen out, and sites 1 and 4 are now nearest neighbours. Due to the fact that the obtained Hamiltonian is of the same form as the original one, we can reiterate the steps successively, meaning we can go back to step (i) and repeat the steps until a point that is determined next. The procedure is illustrated in figure (3.2).

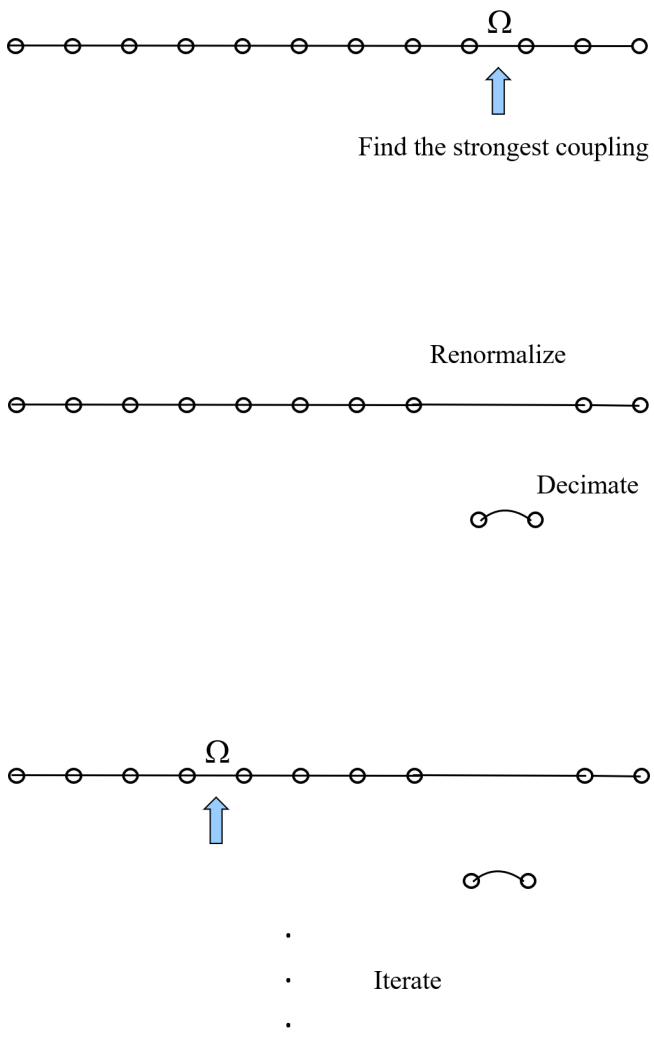

Figure 3.2: Schematic procedure of the SDRG.

The whole idea behind a renormalization group theory is to iterate the decimation procedure until the parameters of the Hamiltonian no longer change upon new iterations. When that happens, we say that we have found a fixed point, from which we can extract the thermodynamic properties of the system (M. E. Fisher, 1974). In 1994, Fisher showed that for the SDRG method applied to the spin-$\frac{1}{2}$ antiferromagnetic chain, all non-trivial initial distributions $P(J)$ have the same fate (D. S. Fisher, 1994):

$$\boxed{P^*(J,\Omega) = \frac{\alpha}{\Omega}\left(\frac{\Omega}{J}\right)^{1-\alpha}} \tag{3.5}$$

with

$$\boxed{\frac{\Delta J}{\langle J\rangle} \to \infty.} \tag{3.6}$$

This means that the distribution gets asymptotically wide and disorder approaches infinity as the distribution approaches its fixed point. This is extremely important for it states that the probability of a decimation occurring in which the bond between $\boldsymbol{S}_1$ and $\boldsymbol{S}_2$ or the bond between $\boldsymbol{S}_3$ with $\boldsymbol{S}_4$ is comparable to the one between $\boldsymbol{S}_2$ and $\boldsymbol{S}_3$ goes to zero as the distribution approaches its fixed point. In other words, the procedure is asymptotically exact, meaning the more we iterate, the more accurate it becomes.

To find the system's physical properties, the SDRG method dictates we iterate the procedure until the energy scale Ω is lowered to match the temperature T. Afterwards, the non-decimated spins are considered free, as in non-interacting, whereas the ones that are paired are considered inert and therefore don't contribute to the thermodynamic quantities to be extracted. Thus, we are left with a system composed only of free spins, therefore the system is easily diagonalized and consequently the physical quantities are promptly obtained (Bhatt and Lee, 1982). This may seem strange at first, but it is justified by the fact that the temperature T of interest is much lower than the initial energy scale Ω_0. Hence the system suffers enough decimations so that the initial distribution $P(J)$ is close to its fixed point $P^*(J)$. In this way, the energy scale of the majority of the interactions between the remaining spins is much lower than the temperature T and the spins are essentially free. The static magnetic susceptibility, χ, for instance, is simply given by the Curie contribution of each of the active spins at temperature T.

$$\chi \sim \frac{n_{\Omega=T}}{T}, \tag{3.7}$$

where $n_{\Omega=T}$ is the fraction of active spins at energy scale Ω. Thus, we are left now with the task of determining $n_{\Omega=T}$.

We start by noting that, in each decimation, 2 spins are removed from the system. This means that the fraction of spins dn_Ω that can be decimated when changing the energy scale of the system from Ω to $\Omega - d\Omega$ is 2 times the fraction of spins available for a decimation multiplied by the probability of a decimation occurring in this specific energy scale, $P(J = \Omega)d\Omega$. Hence,

$$dn_\Omega = 2n_\Omega P(\Omega)d_\Omega. \tag{3.8}$$

We now assume that the distribution $P(J)$ is close to its fixed point, so $P(J)$ is then given by $P^*(J)$, which is a justifiable assumption given that we are interested in the low energy limit and all distributions flow to their fixed point eventually. Thus, if we take $P(J) \sim P^*(J)$ from Eq. (3.5) and make the substitution in Eq. (3.8) we get

$$n_\Omega \sim \frac{1}{\Gamma^2}, \qquad \Gamma = \ln \frac{\Omega_0}{\Omega}. \tag{3.9}$$

Therefore the static magnetic susceptibility, χ, at temperature T is given by

$$\chi \sim \frac{n_{\Omega=T}}{T} \sim \frac{1}{T\Gamma^2_{\Omega=T}}. \tag{3.10}$$

From Eq. (3.5) we can also determine the relation between energy and length scales. It is clear that the average distance between neighbouring active spins tend to grow as we remove spins from the system. This basically means that

$$L_\Omega \sim n_\Omega^{-1}. \tag{3.11}$$

Substituting Eq. (3.11) in Eq. (3.9) we find that the relation between energy and length scales is given by

$$\boxed{\Gamma \sim L_\Omega^\psi, \qquad \psi = \frac{1}{2}}, \tag{3.12}$$

where ψ is called the tunnelling exponent and it dictates an universality class. For the antiferromagnetic Heisenberg chain, the tunnelling exponent was first calculated by Fisher and found to be $\psi = \frac{1}{2}$. The particular relation between energy and length scales depicted in Eq. (3.12) is named activated (exponential) dynamic scaling, and

it is characteristic of systems with an infinite disorder fixed point. These systems are said to flow towards infinite disorder.

One can also choose to iterate the method up to the point where all spins are paired in a singlet state. When this happens, the system is said to be in a random singlet phase, which in turn corresponds to the system's ground state, as illustrated in figure (3.3).

Random Singlet phase

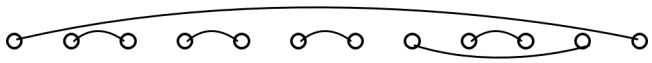

Figure 3.3: Random singlet phase.

We have thus far laid the basic concepts behind the SDRG and presented some immediate theoretic results. These results have been numerically (Hoyos, 2005) and empirically (Masuda et al., 2004) discoursed in other works. Our goal now is to elaborate this method for Majorana fermions in the honeycomb lattice as well as present and discourse our numerical results. It is important to make the remark that from hereafter we are again working with Majorana fermions. Therefore, it is necessary that we redefine the decimation procedure in terms of the Majoranas.

3.2 The Majorana Honeycomb SDRG

We shall now apply the same procedure to a Majorana honeycomb model. As stated in section (2.4), we did so for two different initial distributions of the plaquette operators W_p, which we refer to as the zero flux sector and the random flux sector, following what was done for the Kitaev model. As we shall see, however, the renormalization procedure changes the lattice's connectivity, in such a way that **we can no longer define these plaquette operators in the same manner**. In spite of this, for simplicity, we shall keep referring to the system whose **initial configuration** is $W_p = 1$ for all p as the Majorana honeycomb model in the zero flux sector. Analogously, the random flux sector is used to denote the system when the **initial configuration** is that of $W_p = \pm 1$ randomly and uniformly distributed.

From Eq. (2.37), it follows that each site interacts with its three neighbouring spins according to

$$H = \sum_k (\pm) i t_{jk} \eta_j \eta_k, \tag{3.13}$$

where k accounts for the sum over all three neighbouring spins and the plus-minus sign is due to the fact that the bond between spins has a well-defined direction (in accordance with the operators u_{jk} defined in section (2.2), which can assume the values +1 or −1). The first decimation procedure is illustrated in figure (3.4).

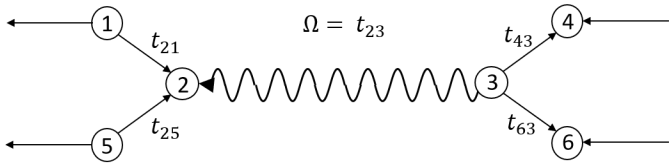

Figure 3.4: Visual representation of all the sites involved in the first decimation procedure. The bond between spins 2 and 3 is found to be the strongest. The bond direction was chosen in this particular way for it is the one which minimizes energy, i.e., it corresponds to the zero flux sector.

Just as we did for the 1/2-spin Heisenberg chain, we take

$$H_1 = i t_{21} \eta_2 \eta_1 + i t_{25} \eta_2 \eta_5 + i t_{43} \eta_4 \eta_3 + i t_{63} \eta_6 \eta_3 \tag{3.14}$$

as a perturbation of

$$H_0 = i t_{23} \eta_2 \eta_3, \tag{3.15}$$

where $\{\eta_j, \eta_k\} = 0$, in accordance with Eq. (2.11). Here we chose the following order for the representation of the interactions:

$$H_{interaction} = + i \ \mid t \mid \ \eta_{receiving} \, \eta_{sending}. \tag{3.16}$$

The correction term in energy which arises from perturbation is given by:

$$\tilde{H} = \frac{1}{E_0 - E_1} \langle 0|H_1|1\rangle\langle 1|H_1|0\rangle. \tag{3.17}$$

Let us rewrite equations (2.12) - (2.15) for practical reasons:

$$\eta_2|0\rangle = (a + a^\dagger)|0\rangle = |1\rangle,$$
$$\eta_3|0\rangle = \frac{a - a^\dagger}{i}|0\rangle = i|1\rangle,$$
$$\eta_2|1\rangle = |0\rangle,$$
$$\eta_3|1\rangle = -i|0\rangle.$$

Here, $|0\rangle$ represents the usual spin-$\frac{1}{2}$ vacuum and $|1\rangle = a^\dagger|0\rangle$. Thus, $H_0|0\rangle = -t_{23}|0\rangle$ and $H_0|1\rangle = +t_{23}|1\rangle$, meaning that $E_0 = -t_{23}$ and $E_1 = +t_{23}$. Next we shall calculate each term of Eq. (3.17) individually.

$$\begin{aligned}\langle 0|H_1|1\rangle &= \langle 0|it_{21}\eta_2\eta_1 + it_{25}\eta_2\eta_5 + it_{43}\eta_4\eta_3 + it_{63}\eta_6\eta_3|1\rangle,\\ &= \langle 0| - it_{21}\eta_1\eta_2 - it_{25}\eta_5\eta_2 + it_{43}\eta_4\eta_3 + it_{63}\eta_6\eta_3|1\rangle,\\ &= \langle 0| - it_{21}\eta_1 - it_{25}\eta_5 + t_{43}\eta_4 + t_{63}\eta_6|0\rangle.\end{aligned} \tag{3.18}$$

$$\begin{aligned}\langle 1|H_1|0\rangle &= \langle 1|it_{21}\eta_2\eta_1 + it_{25}\eta_2\eta_5 + it_{43}\eta_4\eta_3 + it_{63}\eta_6\eta_3|0\rangle,\\ &= \langle 1| - it_{21}\eta_1\eta_2 - it_{25}\eta_5\eta_2 + it_{43}\eta_4\eta_3 + it_{63}\eta_6\eta_3|0\rangle,\\ &= \langle 1| - it_{21}\eta_1 - it_{25}\eta_5 - t_{43}\eta_4 - t_{63}\eta_6|1\rangle.\end{aligned} \tag{3.19}$$

Equation (2.9) states that $\eta_k^2 = 1$, thus:

$$\begin{aligned}\langle 1|\eta_i|1\rangle &= \langle 1|\eta_2^2\eta_i|1\rangle,\\ &= -\langle 1|\eta_2\eta_i\eta_2|1\rangle,\\ &= -\langle 0|\eta_i|0\rangle.\end{aligned} \tag{3.20}$$

Therefore we write:

$$\langle 0|H_1|1\rangle = -it_{21}\eta_1 - it_{25}\eta_5 + t_{43}\eta_4 + t_{63}\eta_6, \tag{3.21}$$
$$\langle 1|H_1|0\rangle = it_{21}\eta_1 + it_{25}\eta_5 + t_{43}\eta_4 + t_{63}\eta_6. \tag{3.22}$$

Substituting this result in equation (3.17) along with what we found for E_0 and E_1, multiplying the terms, and neglecting the constants we finally obtain

$$\boxed{\tilde{H} = i\left(\frac{t_{21}t_{43}}{t_{23}}\right)\eta_4\eta_1 \; + i\left(\frac{t_{21}t_{63}}{t_{23}}\right)\eta_6\eta_1 + i\left(\frac{t_{25}t_{43}}{t_{23}}\right)\eta_4\eta_5 + i\left(\frac{t_{21}t_{63}}{t_{23}}\right)\eta_6\eta_5}. \tag{3.23}$$

Notice how each of the terms in the equation above is precisely of the form

$$H_{ij} = i\tilde{t}\eta_i\eta_j, \qquad \tilde{t} = \frac{t_i t_j}{t_\Omega}, \tag{3.24}$$

where t_Ω is the strongest coupling between active spins in the system, which implies that $\tilde{t} < t_i, t_j$ always, as intended. What this means is that the perturbation basically has the effect of creating weaker, yet new interactions between sites which were initially disconnected. Following the steps defined in section (3.1), we now freeze out sites 2 and 3 and let the effective interaction be given by equation (3.23).

Taking a closer look at equation (3.23), one can see that the sites which were originally attached to the same side of the decimated bond do not form a connection between them, whereas **all** Majoranas which were originally attached to opposite sides of the decimated bond do. This is illustrated in figure (3.5).

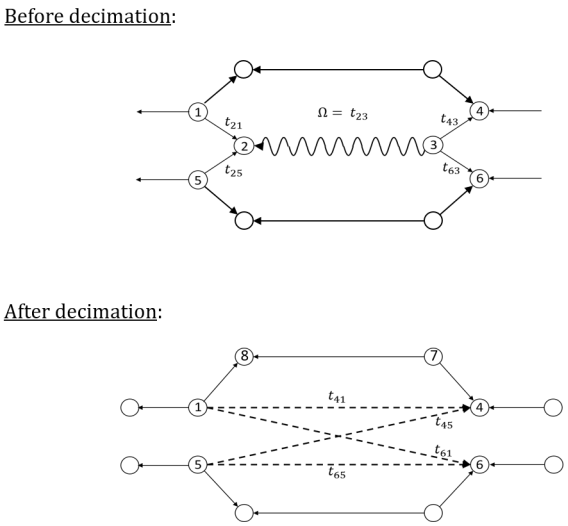

Figure 3.5: Representation of a single decimation in a previously non-decimated system.

Notice how this procedure changes the topology of the system. After the decimations start, the fermionic interactions are no longer restricted to that of a honeycomb lattice, which is already in direct contrast to what happens in the 1-dimensional Heisenberg chain. As stated above, all Majoranas which were originally attached to opposite sides of the decimated bond form a new connection. This means that the number of new bonds created in each decimation is $i \times j$, where i is the number

of sites connected to one side of the decimated bond, and j is the number of sites connected to the other end.

Let us suppose now that at some point $\Omega = t_{41}$, meaning that this bond shall be decimated and all sites connected to site 4 are to form bonds with all sites connected to site 1. However, we see that two of them are already connected, 7 and 8. If we calculate the effective coupling arising from second order perturbation theory in this case, we naturally get the term $i\tilde{t}\eta_8\eta_7$, among others. This term can be factored together with the one that represents the already existing bond between sites 8 and 7, which is part of the system's Hamiltonian, $it_{87}\eta_8\eta_7$. This gives us $i\left(t_{87}+\tilde{t}\right)\eta_8\eta_7$. Thus

$$\tilde{H}_{87} = i\tilde{t}'\eta_8\eta_7, \qquad \tilde{t}' = t_{87} + \tilde{t}. \tag{3.25}$$

This means that whenever a new bond is to be generated where there is already an existing connection, the resulting binding energy is simply given by the direct sum of the energy originated from the already existing bond and the energy that arises from the decimation procedure. This implies that applying the SDRG method to a system composed of N Majorana fermions yields $\sim \boldsymbol{N^3}$ **interactions**.

There are still two remarks left that we wish to make before proceeding into the computational part, and for that we again turn our attention to equation (3.23). The Majorana fermion honeycomb model consists of a bipartite system, for it can in turn be seen as two triangular Bravais lattices, which we have been referring to as "even" and "odd". Initially, the odd sites are connected **only** to the even sites, and vice versa, as can be seen in figure (2.1). As stated before, equation (3.23) shows us that there are no arising connections between sites which were originally attached to the same side of a decimated bond, hence there is no "odd"-"odd" connection, nor there is an "even"-"even" connection. Therefore the decimation procedure **preserves the bipartite structure** of the system.

The other very important aspect we wish to point out is that the aforementioned procedure was illustrated for a very specific case, the one in which all initial bonds point in the direction of the even sites. This initial configuration, besides representing the zero flux sector, also possesses a peculiar property. All even sites will **always** be on the receiving end of the bonds, even when the SDRG completely changes

the system's connectivity. This is not true, however, for a different initial bond configuration. Figure (3.6) shows how the direction of the arising bond is related to the initial bond configuration.

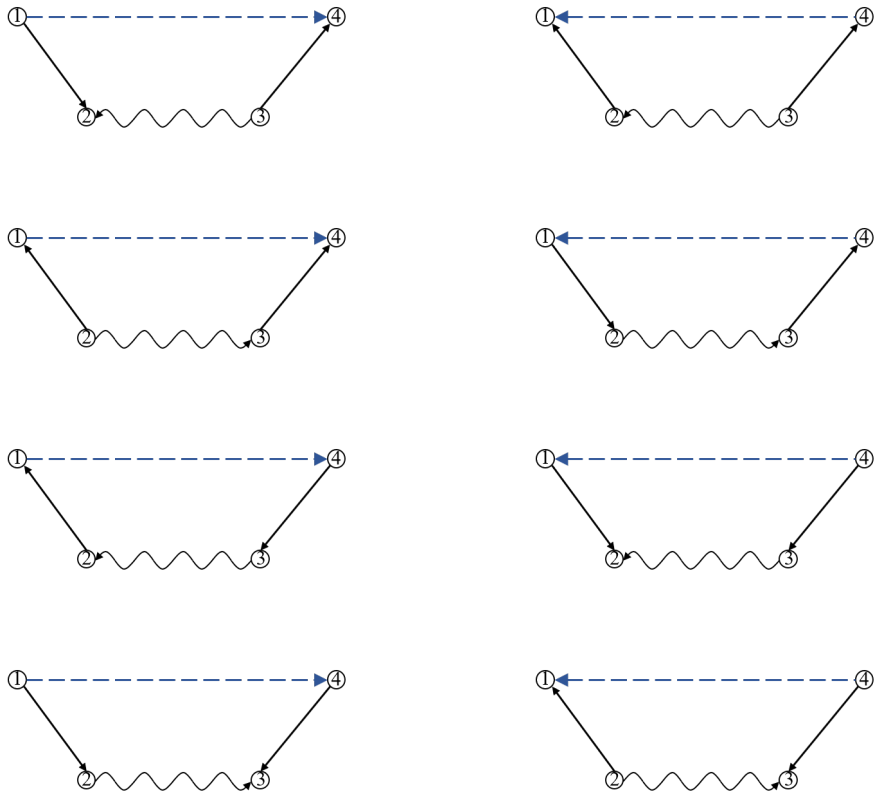

Figure 3.6: Every possible initial bond configuration which influences the direction of the arising bond. The wavy arrows represent Ω, while the blue ones represent the direction of the new bond, resultant of perturbation.

Chapter 4

ALGORITHM AND RESULTS

4.1 The zero flux sector

We now discuss our findings for the disordered Majorana honeycomb model. We started by generating the honeycomb lattice with randomly assigned coupling constants distributed according to an uniform distribution, i.e.

$$P(t) = 1, \quad t \in (0, 1). \tag{4.1}$$

We then fixed $W_p = 1$ for all plaquettes, and therefore focused on the zero flux sector. The choice for the bond configuration which upholds $W_p = 1$ for all plaquettes was $u_{jk} = 1$ for all links, where j belongs to the even sublattice and k belongs to the odd sublattice, just as was done for the Kitaev model (figure 4.1). Following our choice of representation (equation 3.16), the Hamiltonian which describes this initial condition is given by Eq. (4.2).

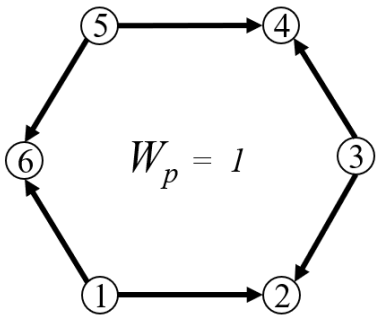

Figure 4.1: Representation of a single plaquette. All even sites are on the receiving end of the bonds.

$$H = \sum_{n.n.} + i \ | t | \eta_{even} \eta_{odd}. \tag{4.2}$$

Our goal then was to use the SDRG method to determine how energy relates to the number of active Majoranas, for this way we can work out a relation similar to equation (3.12). The obtained result for a system of 1128 Majoranas is shown in figure (4.2).

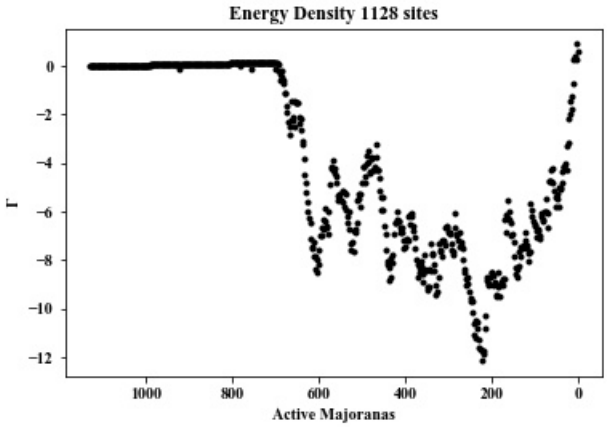

Figure 4.2: System composed of 1128 Majorana fermions. $\Gamma = \ln \frac{\Omega_0}{\Omega}$.

The method raises the system's energy scale, meaning the SDRG seems inadequate to study the system under these initial conditions.

In an attempt to verify if the observed behaviour is a consequence of the system size, we aimed to reduce computational time and thus work with increased system sizes. The idea was to reduce the $\sim N^3$ interactions that the SDRG for the Majorana honeycomb model yields. We asked ourselves if we could keep track of only some k greatest bonds for each site and obtain the same energetic result for each step of the decimation, up to the random singlet phase, this way reducing the number of interactions to $\sim kN^2$ (figure 4.3).

For a given initial configuration of a system composed of 1128 sites, we found that cutoff number to be $k = 70$. What was left to see was how this number would change upon new realizations of the program and how it relates to system size. Our findings can be seen in figure (4.4).

From thereafter, using that result, we expanded the system's size and always worked above the cutoff value, in order to obtain the same energetic result as if we were applying the exact decimation procedure. We then reran the simulation for a system composed of 4186 Majoranas under the same initial conditions, i.e., zero flux sector and t uniformly distributed, with $k = 300$ (figure 4.5).

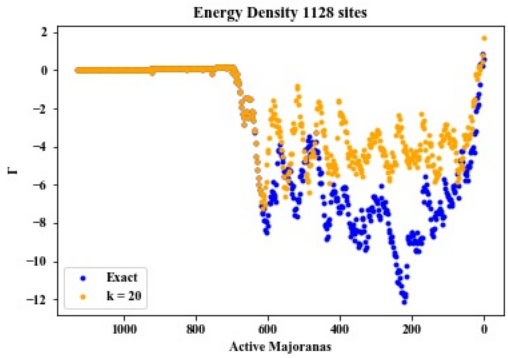

(a)

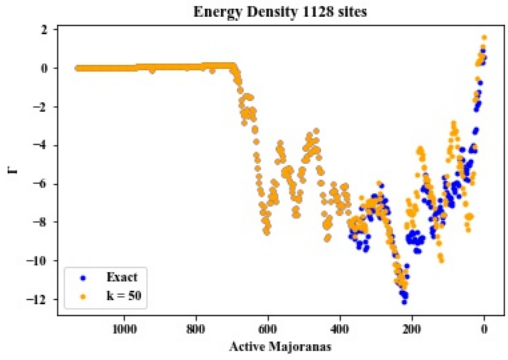

(b)

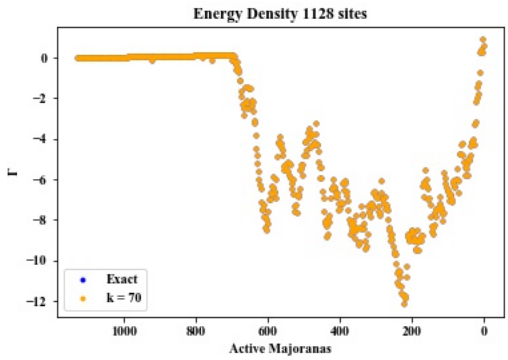

(c)

Figure 4.3: System composed of 1128 Majorana fermions. In each realization we tested a number k above which there is a cutoff and the weaker connections of a site are discarded so as to only keep track of the k greatest bonds. e.g.: if the cutoff $k = 40$ and a site is about to go from 30 connections to 50 connections, we discard the 10 weakest interactions and that site is left with only the 40 strongest bonds. (a)$k = 20$. (b)$k = 50$. (c)$k = 70$.

The system's energy scale increases even more! We are thus led to believe that this behaviour is not consequence of system size and hence the method is inadequate

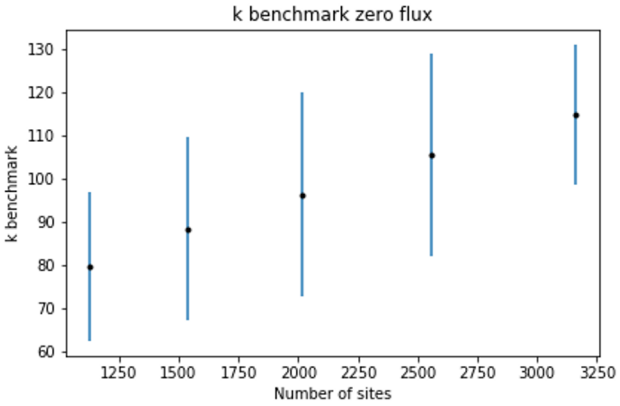

Sites	Realizations
1128	300
1540	200
2016	150
2556	100
3160	30

Figure 4.4: Cutoff value k for a given system size. For each size multiple program realizations were made.

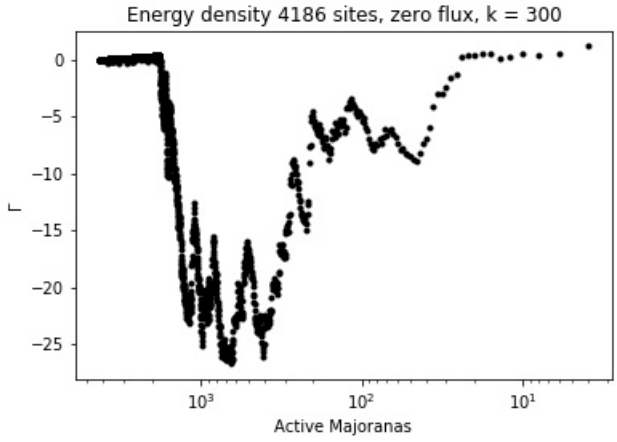

Figure 4.5: System composed of 4186 Majoranas. The method still raises the system's energy scale.

given these initial conditions. In trying to understand this, we supposed that the behaviour is due to bad decimations, meaning that the system cannot get through the initial regime where the distribution of t is not yet broad, in a manner that the distribution does not flow to the neighbourhood of its fixed point. To test this hypothesis, we increased the initial disorder so that the system may be able to cross the initial regime resulting in the decimations becoming asymptotically exact. This was done by changing the initial distribution $P(t)$ to

$$P(t) = \alpha \frac{1}{t^{1-\alpha}}, \quad t \in (0,1), \quad \alpha > 0. \tag{4.3}$$

It follows that *smaller α* $\rightarrow$ *Stronger disorder* (appendix A). Our goal then was to find α, if there was one, for which the energy scale only diminished while still in the zero flux sector

To search for a critical value for α, we worked with a fixed system size N, started with $\alpha = 1$ and systematically decreased it by 0.01 each simulation, thus increasing the disorder in the initial distribution every time. We actually relaxed the condition for Γ in a manner that we demanded that

$$\Gamma < 1.5\Gamma_0, \tag{4.4}$$

to account for the fact that there can be some bad decimations in the initial regime, given that the method is suited to study the physics in the low energy limit, where the decimations need to be asymptotically exact. The result obtained for a system composed of 4186 sites, with $\alpha = 0.30$, is displayed in figure (4.6).

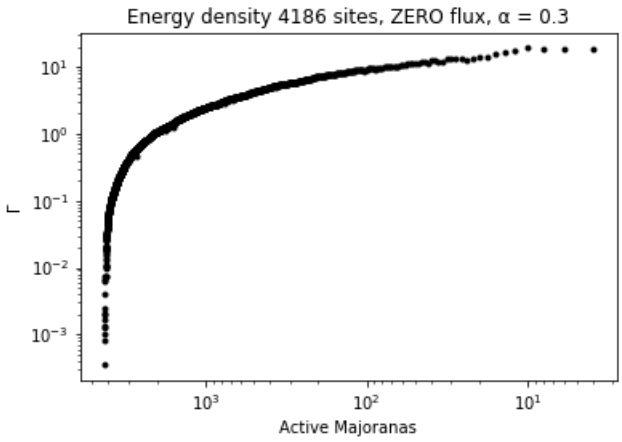

Figure 4.6: System composed of 4186 Majoranas. The method seems adequate given the initial condition $\alpha = 0.30$. We suppose that the difference in behaviour near the end of the decimations is due to finite system size; since we are interested in the thermodynamic limit, this wouldn't be a problem.

Figure (4.6) implies that there is a critical value of α, given that initial configuration, for which the method reduces the system's energy scale. To see how this reflects in the distribution of t we take a look at the distributions in both cases, i.e., $\alpha = 1$ and $\alpha = 0.30$ for the system composed of 4186 Majoranas (figure 4.8).

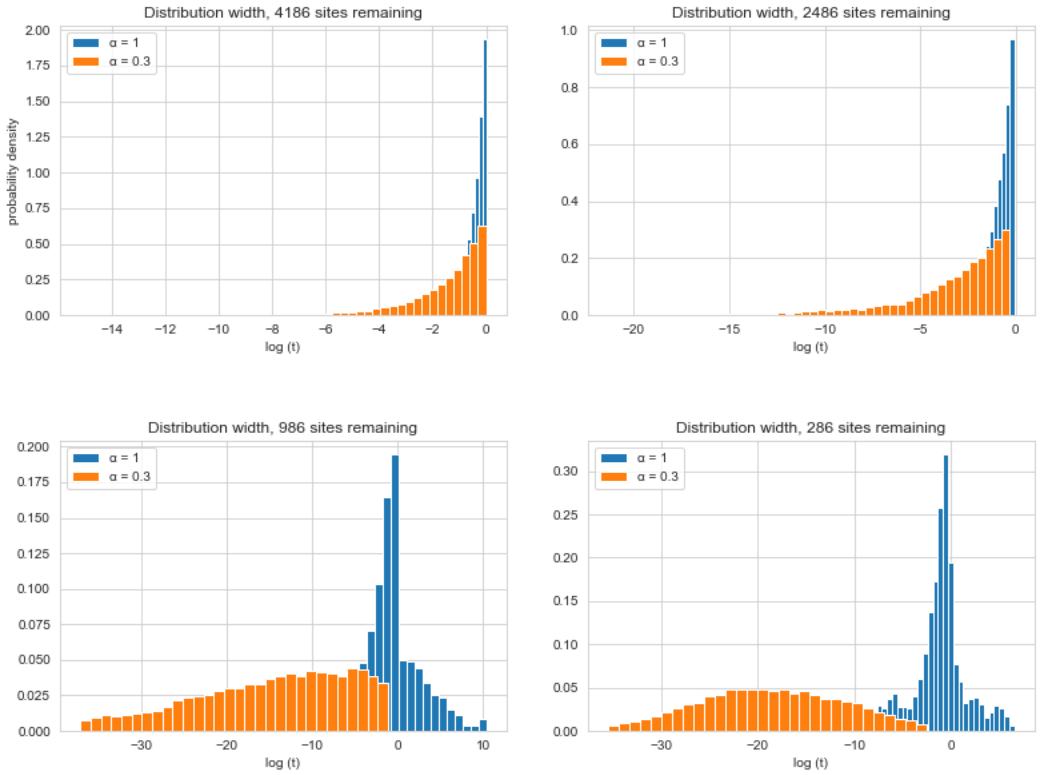

Figure 4.8: Distribution flow for a system composed of 4186 Majoranas under two different initial disorders, $\alpha = 1$ and $\alpha = 0.3$.

We observe, in figure 4.8, how wider the distribution for $\alpha = 0.3$ gets as we iterate the decimation procedure in comparison with the distribution for $\alpha = 1$. Of course, the initial distribution for $\alpha = 0.3$ is already broader, as expected. However the difference in growth strongly suggests that our proposition is correct. The system with $\alpha = 1$ cannot get through the initial regime where $P(t)$ is not yet wide and the distribution doesn't flow to the neighbourhood of its fixed point. Whereas the wide distribution for $\alpha = 0.3$ suggests that the system does flow to the neighbourhood of its fixed point and the method is adequate for studying the effects of disorder under these initial conditions **as long as the result is extendible to the thermodynamic limit**.

To determine whether obtained results for a reduced system size can be extended to the thermodynamic limit, we need first to determine how α relates to system size. Our findings can be seen in figure (4.9).

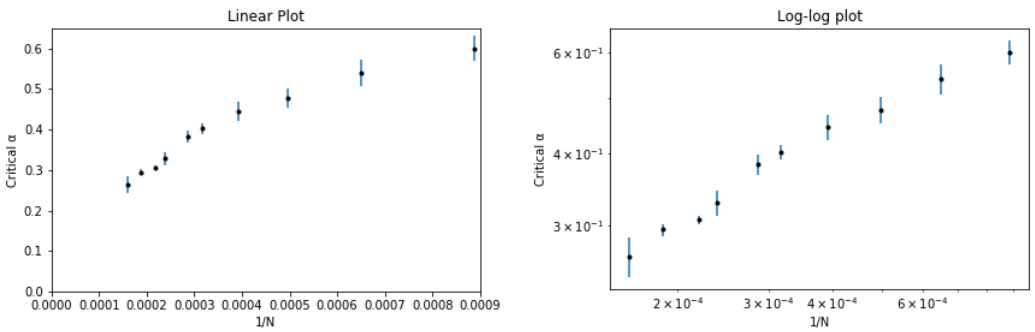

Figure 4.9: Two plots for the necessary α so that the method actually diminishes the system's energy scale. In order to check for a power law dependency we did a log-log plot. From these we extrapolate the behaviour for $N \to \infty$ to determine how disorder affects the system in the thermodynamic limit.

We observe that the relation between α and $1/N$ is approximately linear above a certain system size. We argue that the realizations for smaller systems are inaccurate, for the distribution does not have enough time to be sufficiently wide and consequently the result is heavily influenced by the finiteness of the system. That being said, we considered only systems with $N > 3000$, and extrapolated α as $N \to \infty$ (figure 4.10).

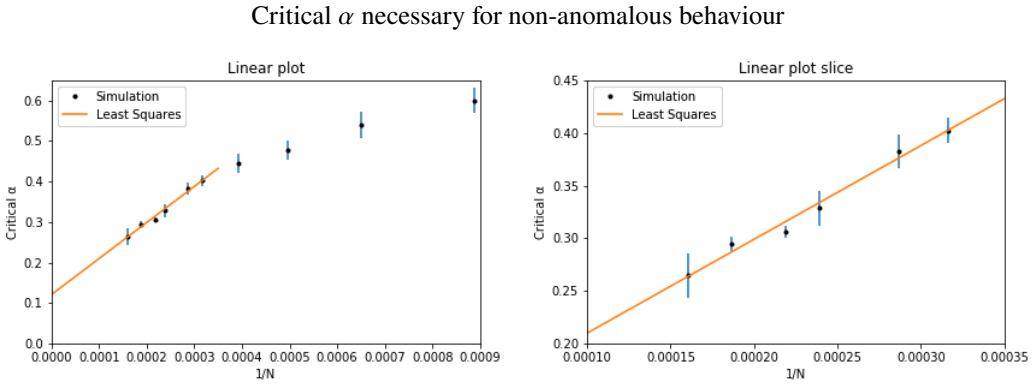

Figure 4.10: Linear fitting for the critical α considering only systems where $N > 3000$. The second plot consists of a close up of the considered data, and was done to better see how well the linear fitting adjusts the data.

If this relation is indeed maintained as $N \to \infty$, then $\alpha \nrightarrow 0$. This means that there is a value of α below which the system **always** flows to infinite disorder. Our results suggest that this value is $\alpha = 0.12 \pm 0.02$. Consequently, the Majorana honeycomb model in the zero flux sector will always flow to infinite disorder given that the initial

disorder is strong enough, whereas the symmetry somehow protects the system from weak disorder; a symmetry which arises from making all $W_p = 1$ and thus imposing specific directions for each bond. This is analogous to the Haldane phase, in which a gap shields the system from weak disorder in a spin-1 antiferromagnetic Heisenberg chain.

4.2 The random flux regime

We now turn our attention to the random flux regime, this means the plaquettes are no longer restricted to $W_p = 1$ (figure 4.11). It is extremely important to remark that an uniform distribution of W_p was used, meaning that for roughly half of the plaquettes $W_p = 1$, while for the other half $W_p = -1$. This corresponds to a highly excited initial state.

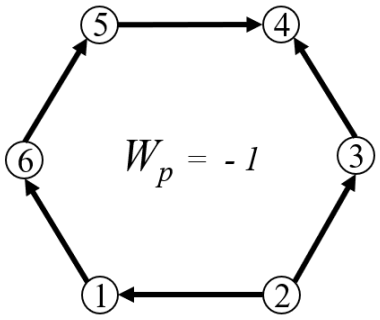

Figure 4.11: Possible plaquette configuration.

Following our choice of representation (equation 3.16), the Hamiltonian which encloses this initial condition is

$$H = \sum_{n.n.} \pm \mid t \mid \eta_{even}\, \eta_{odd}. \tag{4.5}$$

We chose to work with the distribution from Eq. (4.3), yet starting with $\alpha = 1$, thus using a uniform distribution for the initial tests. Again, our goal was to analyse how energy relates to the number of active Majoranas. To do this, we first determined a cutoff value k just like was done for the zero flux case:

Afterwards, we applied the initial condition described above, i.e., $\alpha = 1$, and ran the simulation for a system composed of 4186 Majoranas while maintaining

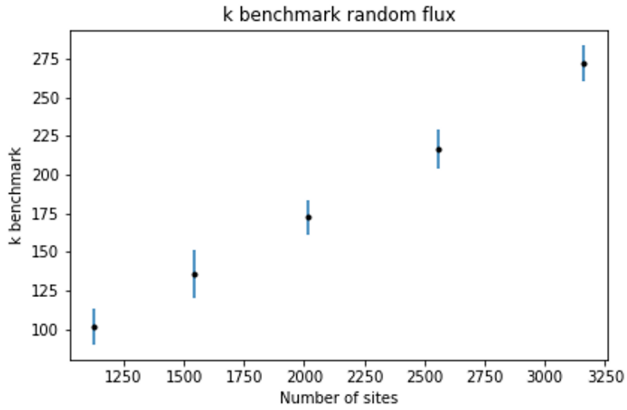

Sites	Realizations
1128	200
1540	150
2016	100
2556	50
3160	20

Figure 4.12: Cutoff value k for the number of bonds to be considered for each site so as to get the exact result. We can clearly see that k is better defined for the random flux case.

$k = 500$. We observed that energy relates to the number of active sites in the manner shown in figure (4.13).

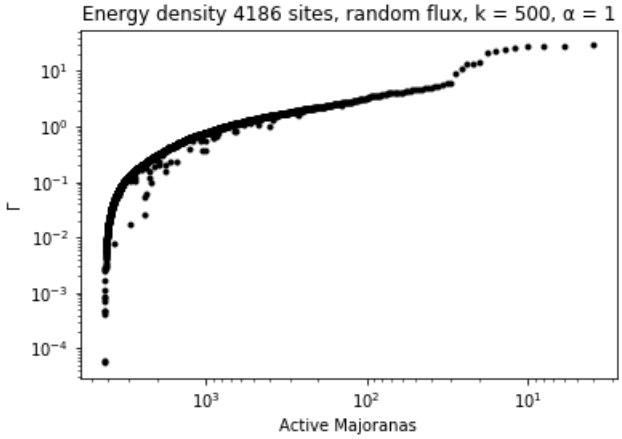

Figure 4.13: System composed of 4186 Majoranas, for a random flux configuration and an uniform initial distribution. Some bad decimations happen in the initial regime, as can be seen by the large fluctuations at the early stages of the procedure, but they quickly disappear in the low energy limit. The anomalous behaviour at the end is believed to be the effect of a finite system.

The method seems to work as intended, lowering the system's energy scale even for an uniform initial distribution. Indeed, by checking the distribution flow figure (4.14), we see that disorder grows asymptotically, thus we say that the system flows to infinite disorder and therefore an activated dynamic scaling behaviour, similar to

equation (3.12), is to be verified. But first, one can wonder what would be the effect of increasing the initial disorder. To test that, we reran the simulation with $\alpha = 0.3$ (figure 4.15).

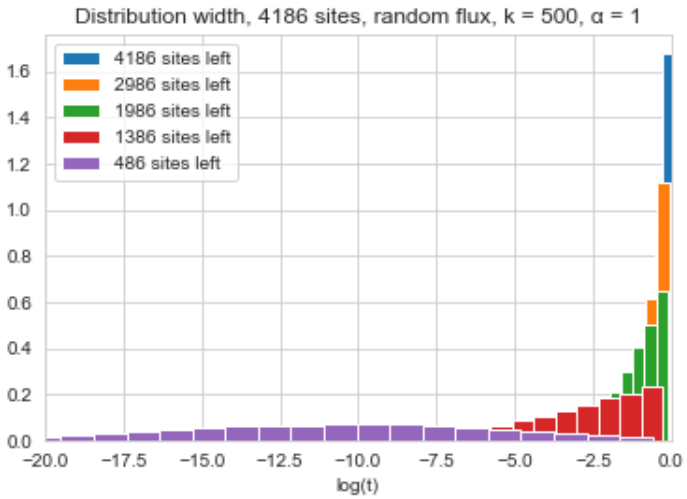

Figure 4.14: Distribution width for different stages of the decimation procedure given an uniform initial distribution.

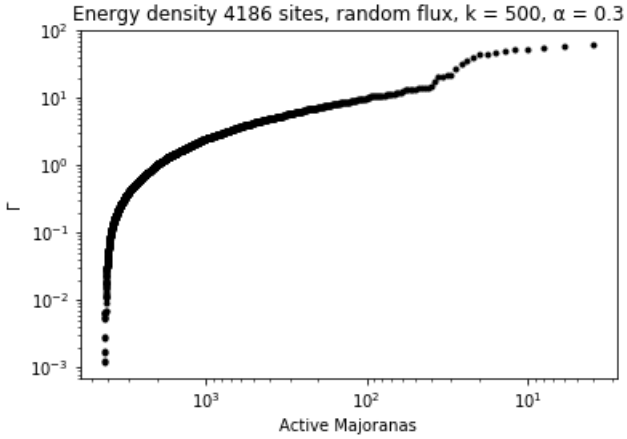

Figure 4.15: Energy density given a stronger initial disorder. Bad decimations can no longer be seen at the early stages of the procedure, but the anomalous behaviour at the end remains.

The system gets through the initial regime faster and the decimations become asymptotically exact sooner, as can be seen by the distribution flow in figure (4.16).

If this influences a system's properties in the thermodynamic limit is discussed next, when we calculate the tunnelling exponent ψ for both cases.

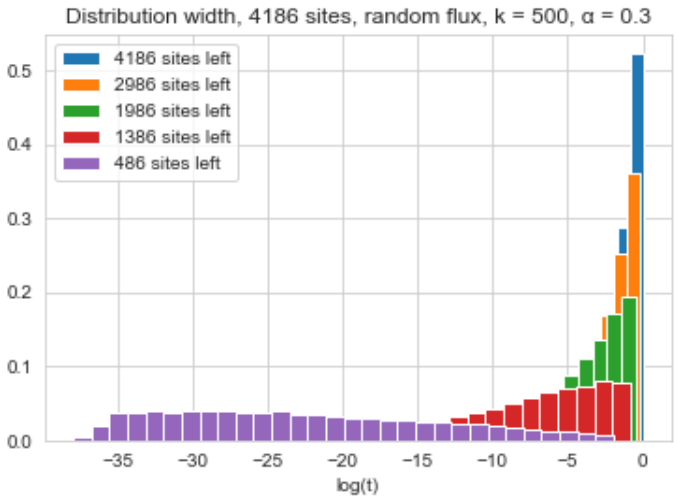

Figure 4.16: Distribution width for different stages of the decimation procedure given a stronger initial disorder.

To calculate ψ, we considered the interval of decimations for which the system is assumed to be close to its fixed point but sufficiently distant from the last decimations so as to avoid the effects of a finite sized system. Figure (4.17) shows our findings for a system composed of 4186 Majoranas, both for $\alpha = 1$ and for $\alpha = 0.3$.

For both cases we found ψ to be fairly close to the one calculated by Fisher for the antiferromagnetic Heisenberg chain, i.e., $\psi = 1/2$. This exponent dictates an universality class, and is not in any way restricted to $\psi = 1/2$. We strongly believe that the Majorana honeycomb model in the random flux regime always flows to infinite disorder, with a tunnelling exponent $\psi = 1/2$. The effect of a stronger initial disorder, i.e., a broader initial distribution, is believed to only affect how fast the procedure becomes asymptotically exact. Given that we are interested in the low energy limit, this difference in initial configuration is presumed to be neglectable in the thermodynamic limit. Further testings with increased system size should be done to corroborate the hypothesis. In the future, we wish to vary the distribution of W_p in order to see how it affects these results.

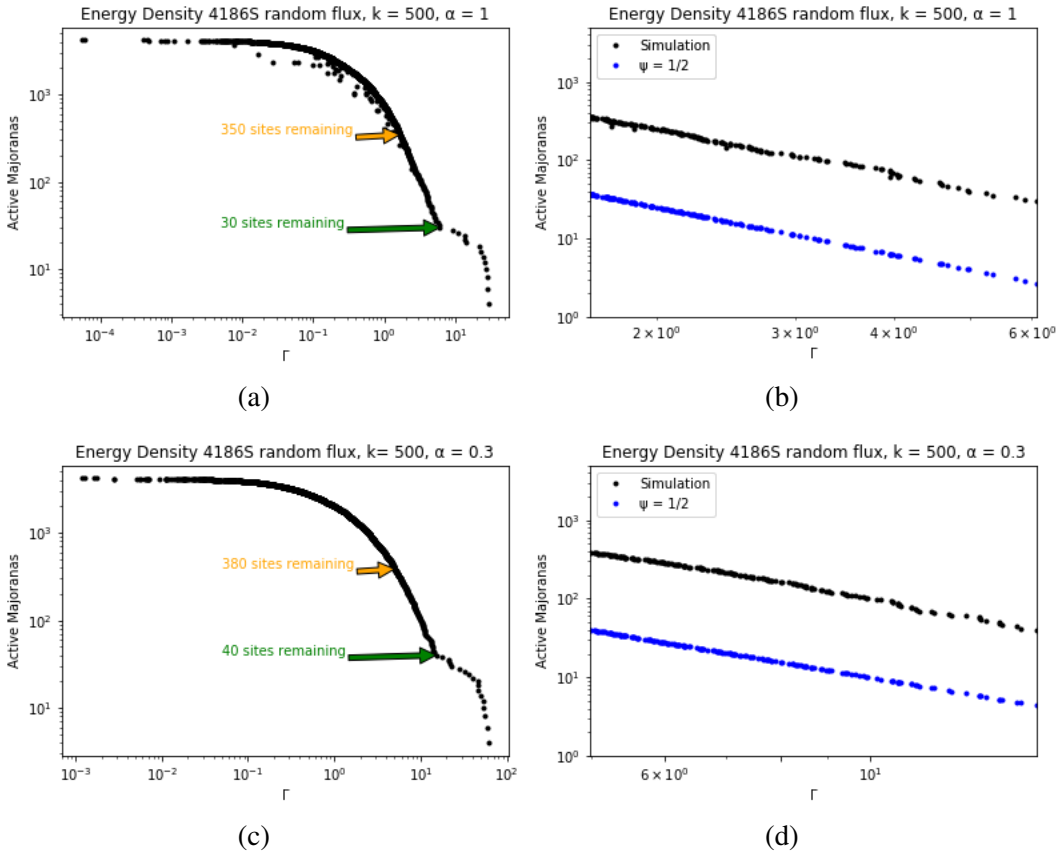

Figure 4.17: System composed of 4186 Majorana fermions. The upper panel corresponds to $\alpha = 1$, while the second one to $\alpha = 0.30$. (b) and (d) represent, respectively, the slice of (a) and (c) considered in the calculation of ψ. (b) $\psi = \frac{1}{1.90}$. (d) $\psi = \frac{1}{2.04}$.

4.3 The square lattice

Lastly, we present a brief result for the Majorana square lattice. It follows in figure (4.18), a program realization for a system composed of 3136 Majoranas for $\alpha = 1$. The bond directions were randomly attributed, so this would be analogous to the random flux regime.

The method lowers the system's energy scale even for $\alpha = 1$, but it is clear that bad decimations happen more often when in comparison with the honeycomb model. We take this to be the consequence of a higher initial connectivity, i.e., each site is connected to 4 other sites, meaning the probability of a bad decimation occurring is higher. Consequently, testings with increased system size should yield more accurate results. This shall be done in the future.

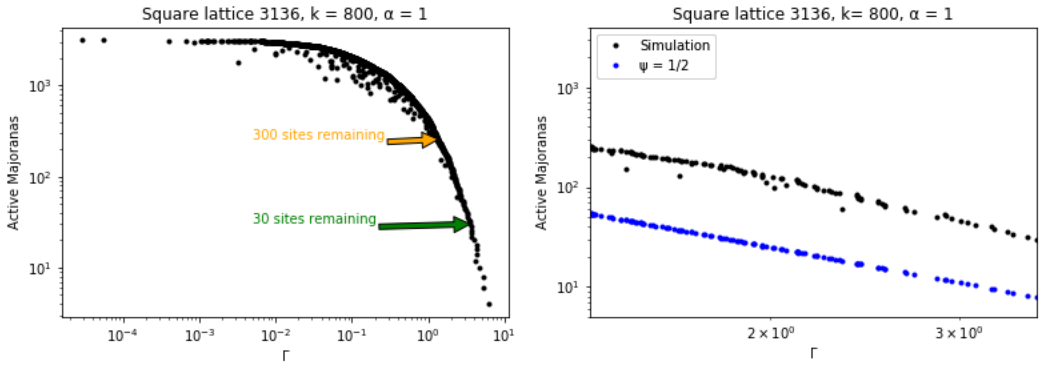

Figure 4.18: The Majorana square lattice composed of 3136 sites. For this case we found $\psi = \frac{1}{2.14}$. We took $k = 800$ as a benchmark hasn't been done for the square lattice yet.

Chapter 5

CONCLUSIONS

In this work we discussed the effects of disorder on a Majorana honeycomb model. For this study the method of choice was the Strong Disorder Renormalization Group (SDRG), first introduced by Ma, Dasgupta and Hu in order to study the low energy physics of a spin-$\frac{1}{2}$ antiferromagnetic Heisenberg chain in the presence of disorder. We started by fixing the initial state of the plaquette variables W_p in a specific configuration which corresponds to the sector containing the ground state, i.e., the zero flux sector. Our findings suggest that the Majorana honeycomb model in the zero flux sector is shielded against weak disorder, whereas the system always flows to infinite disorder given that the initial disorder is strong enough (figure 4.10). We do not know the reasoning behind this, but we suppose the symmetry somehow protects the system from weak disorder; a symmetry which arises from making all $W_p = 1$ and thus imposing specific directions for each bond. This is analogous to the Haldane phase, in which a gap shields the system from weak disorder in a spin-1 antiferromagnetic Heisenberg chain.

We then uniformly randomized W_p in a manner that for roughly half of the plaquettes $W_p = 1$, while for the other half $W_p = -1$, which corresponds to a highly excited initial state. By analysing the distribution width of $P(t)$ during the decimation procedure, we concluded that the Majorana honeycomb model always flows to infinite disorder, even for a uniform initial distribution (figures 4.13, 4.14). We also determined the tunnelling exponent ψ for such systems through the relation between energy density and the fraction of active fermions and found it to be $\psi \sim \frac{1}{2}$ (figure 4.17). Moreover, we presented a brief result for the Majorana square lattice (figure 4.18). The system appears to flow to infinite disorder, however further testings are necessary for conclusive results.

In the future, we aim to increase system size to further corroborate our hypothesis, not only for the honeycomb model but also for the square lattice. We also seek to vary the distribution of W_p in order to see how it affects these results.

Appendix A

HOW α RELATES TO DISORDER

Let us calculate $\frac{\Delta t}{\langle t \rangle}$ so as to determine how the dispersion of $P(t)$ relates to α. The distribution in question is that of Eq. (4.3), i.e.,

$$P(t) = \alpha \frac{1}{t^{1-\alpha}}, \quad t \in (0,1), \quad \alpha > 0, \tag{A.1}$$

$$\langle t \rangle = \int_0^1 t\alpha \frac{1}{t^{1-\alpha}} dt = \frac{\alpha}{1+\alpha}. \tag{A.2}$$

$$\Delta t = \sqrt{\int_0^1 t^2 \alpha \frac{1}{t^{1-\alpha}} dt - \langle t \rangle^2} = \sqrt{\frac{\alpha}{2+\alpha} - \left(\frac{\alpha}{1+\alpha}\right)^2}. \tag{A.3}$$

Therefore,

$$\frac{\Delta t}{\langle t \rangle} = \frac{\sqrt{\frac{\alpha}{2+\alpha} - \left(\frac{\alpha}{1+\alpha}\right)^2}}{\frac{\alpha}{1+\alpha}} = \sqrt{\frac{1}{\alpha(2+\alpha)}}. \tag{A.4}$$

Consequently, the smaller the value of α is, the greater is the dispersion, i.e., the greater is the initial disorder.

BIBLIOGRAPHY

Anderson, P. W. (Mar. 1958). "Absence of Diffusion in Certain Random Lattices". In: *Phys. Rev.* 109 (5), pp. 1492–1505. DOI: https://doi.org/10.1103/PhysRev.109.1492.

– (1973). "Resonating valence bonds: A new kind of insulator?" In: *Materials Research Bulletin* 8.2, pp. 153–160. DOI: https://doi.org/10.1016/0025-5408(73)90167-0.

– (1987). "The Resonating Valence Bond State in La2CuO4 and Superconductivity". In: *Science* 235.4793, pp. 1196–1198. DOI: 10.1126/science.235.4793.1196.

Balents, Leon (2010). "Spin liquids in frustrated magnets". In: *Nature* 464, pp. 199–208. DOI: https://doi.org/10.1038/nature08917.

Banerjee, A. et al. (Apr. 2016). "Proximate Kitaev quantum spin liquid behaviour in a honeycomb magnet". In: *Nature Materials* 15.7, pp. 733–740. DOI: https://doi.org/10.1038/nmat4604.

Bednorz, J. G. and K. A. Müller (1986). "Possible highTc superconductivity in the Ba-La-Cu-O system". In: *Zeitschrift für Physik B Condensed Matter* 64, pp. 189–193. DOI: https://doi.org/10.1007/BF01303701.

Bhatt, R. N. and P. A. Lee (Feb. 1982). "Scaling Studies of Highly Disordered Spin-½ Antiferromagnetic Systems". In: *Phys. Rev. Lett.* 48 (5), pp. 344–347. DOI: 10.1103/PhysRevLett.48.344.

Fisher, Daniel S. (Aug. 1994). "Random antiferromagnetic quantum spin chains". In: *Phys. Rev. B* 50 (6), pp. 3799–3821. DOI: 10.1103/PhysRevB.50.3799.

Fisher, Michael E. (Oct. 1974). "The renormalization group in the theory of critical behavior". In: *Rev. Mod. Phys.* 46 (4), pp. 597–616. DOI: 10.1103/RevModPhys.46.597.

Griffiths, Robert B. (July 1969). "Nonanalytic Behavior Above the Critical Point in a Random Ising Ferromagnet". In: *Phys. Rev. Lett.* 23 (1), pp. 17–19. DOI: https://doi.org/10.1103/PhysRevLett.23.17.

He, Qing Lin et al. (July 2017). "Chiral Majorana fermion modes in a quantum anomalous Hall insulator-superconductor structure". In: *Science (New York, N.Y.)* 357.6348. DOI: 10.1126/science.aag2792.

Hoyos, José A. (Nov. 2005). "Sistemas Quânticos de Spins Desordenados". PhD thesis. Universidade Estadual de Campinas. URL: http://repositorio.unicamp.br/jspui/handle/REPOSIP/277691.

Iglói, Ferenc and Cécile Monthus (2005). "Strong disorder RG approach of random systems". In: *Physics Reports* 412.5, pp. 277–431. DOI: 10.1016/j.physrep.2005.02.006.

Kitaev, Alexei (Jan. 2006). "Anyons in an exactly solved model and beyond". In: *Annals of Physics* 321.1, pp. 2–111. DOI: 10.1016/j.aop.2005.10.005.

Kovács, István A. and Ferenc Iglói (May 2011). "Infinite-disorder scaling of random quantum magnets in three and higher dimensions". In: *Physical Review B* 83.17. DOI: 10.1103/PhysRevB.83.174207.

Lieb, E. H. (1994). "Flux phase of the half-filled band". In: *Phys. Rev. Lett* 73, pp. 2158–2161. DOI: 10.1103/PhysRevLett.73.2158.

Ma, Shang-keng, Chandan Dasgupta, and Chin-kun Hu (Nov. 1979). "Random Antiferromagnetic Chain". In: *Phys. Rev. Lett.* 43 (19), pp. 1434–1437. DOI: 10.1103/PhysRevLett.43.1434.

Majorana, E. (1937). "Teoria simmetrica dell'elettrone e del positrone". In: *Nuovo Cim* 14, pp. 171–184. DOI: https://doi.org/10.1007/BF02961314.

Masuda, T. et al. (Aug. 2004). "Dynamics and Scaling in a Quantum Spin Chain Material with Bond Randomness". In: *Phys. Rev. Lett.* 93 (7), p. 077206. DOI: 10.1103/PhysRevLett.93.077206.

Quito, V. L., José A. Hoyos, and E. Miranda (Aug. 2016). "Random SU(2)-symmetric spin-S chains". In: *Phys. Rev. B* 94 (6), p. 064405. DOI: 10.1103/PhysRevB.94.064405.

Savary, Lucile and Leon Balents (Nov. 2016). "Quantum spin liquids: a review". In: *Reports on Progress in Physics* 80.1, p. 016502. DOI: https://doi.org/10.1088/0034-4885/80/1/016502.

Wilczek, Frank (Sept. 2009). "Majorana returns". In: *Nature Physics* 5, pp. 614–618. DOI: 10.1038/nphys1380.